The production of neutral kaons in Z^0 decays and their Bose-Einstein correlations

The OPAL Collaboration

Abstract

The production of neutral kaons in e^+e^- annihilation at centre-of-mass energies in the region of the Z^0 mass and their Bose-Einstein correlations are investigated with the OPAL detector at LEP. A total of about 1.25×10^6 Z^0 hadronic decay events are used in the analysis. The production rate of K^0 mesons is found to be $1.99 \pm 0.01 \pm 0.04$ per hadronic event, where the first error is statistical and the second systematic. Both the rate and the differential cross section for K^0 production are compared to the predictions of Monte Carlo generators. This comparison indicates that the fragmentation is too soft in both JETSET and HERWIG. Bose-Einstein correlations in $K_S^0 K_S^0$ pairs are measured through the quantity Q, the four momentum difference of the pair. A threshold enhancement is observed in $K_S^0 K_S^0$ pairs originating from a mixed sample of $K^0 \bar{K}^0$ and $K^0 K^0$ ($\bar{K}^0 \bar{K}^0$) pairs. For the strength of the effect and for the radius of the emitting source we find values of $\lambda = 1.14 \pm 0.23 \pm 0.32$ and $R_0 = (0.76 \pm 0.10 \pm 0.11$) fm respectively. The first error is statistical and the second systematic.

To be submitted to Z. Phys. C...

The OPAL Collaboration

R. Akers[16], G. Alexander[23], J. Allison[16], K. Ametewee[25], K.J. Anderson[9], S. Arcelli[2], S. Asai[24], D. Axen[29], G. Azuelos[18,a], A.H. Ball[17], E. Barberio[26], R.J. Barlow[16], R. Bartoldus[3], J.R. Batley[5], G. Beaudoin[18], A. Beck[23], G.A. Beck[13], C. Beeston[16], T. Behnke[27], K.W. Bell[20], G. Bella[23], S. Bentvelsen[8], P. Berlich[10], S. Bethke[32], O. Biebel[32], I.J. Bloodworth[1], P. Bock[11], H.M. Bosch[11], M. Boutemeur[18], S. Braibant[12], P. Bright-Thomas[25], R.M. Brown[20], A. Buijs[8], H.J. Burckhart[8], R. Bürgin[10], C. Burgard[27], N. Capdevielle[18], P. Capiluppi[2], R.K. Carnegie[6], A.A. Carter[13], J.R. Carter[5], C.Y. Chang[17], C. Charlesworth[6], D.G. Charlton[1,b], S.L. Chu[4], P.E.L. Clarke[15], J.C. Clayton[1], S.G. Clowes[16], I. Cohen[23], J.E. Conboy[15], O.C. Cooke[16], M. Cuffiani[2], S. Dado[22], C. Dallapiccola[17], G.M. Dallavalle[2], C. Darling[31], S. De Jong[12], L.A. del Pozo[8], H. Deng[17], M. Dittmar[4], M.S. Dixit[7], E. do Couto e Silva[12], J.E. Duboscq[8], E. Duchovni[26], G. Duckeck[8], I.P. Duerdoth[16], U.C. Dunwoody[5], J.E.G. Edwards[16], P.A. Elcombe[5], P.G. Estabrooks[6], E. Etzion[23], H.G. Evans[9], F. Fabbri[2], B. Fabbro[21], M. Fanti[2], P. Fath[11], M. Fierro[2], M. Fincke-Keeler[28], H.M. Fischer[3], P. Fischer[3], R. Folman[26], D.G. Fong[17], M. Foucher[17], H. Fukui[24], A. Fürtjes[8], P. Gagnon[6], A. Gaidot[21], J.W. Gary[4], J. Gascon[18], N.I. Geddes[20], C. Geich-Gimbel[3], S.W. Gensler[9], F.X. Gentit[21], T. Geralis[20], G. Giacomelli[2], P. Giacomelli[4], R. Giacomelli[2], V. Gibson[5], W.R. Gibson[13], J.D. Gillies[20], J. Goldberg[22], D.M. Gingrich[30,a], M.J. Goodrick[5], W. Gorn[4], C. Grandi[2], E. Gross[26], J. Hagemann[27], G.G. Hanson[12], M. Hansroul[8], C.K. Hargrove[7], P.A. Hart[9], M. Hauschild[8], C.M. Hawkes[8], E. Heflin[4], R.J. Hemingway[6], G. Herten[10], R.D. Heuer[8], J.C. Hill[5], S.J. Hillier[8], T. Hilse[10], P.R. Hobson[25], D. Hochman[26], R.J. Homer[1], A.K. Honma[28,a], R. Howard[29], R.E. Hughes-Jones[16], P. Igo-Kemenes[11], D.C. Imrie[25], A. Jawahery[17], P.W. Jeffreys[20], H. Jeremie[18], M. Jimack[1], M. Jones[6], R.W.L. Jones[8], P. Jovanovic[1], C. Jui[4], D. Karlen[6], J. Kanzaki[24], K. Kawagoe[24], T. Kawamoto[24], R.K. Keeler[28], R.G. Kellogg[17], B.W. Kennedy[20], B. King[8], J. King[13], J. Kirk[29], S. Kluth[5], T. Kobayashi[24], M. Kobel[10], D.S. Koetke[6], T.P. Kokott[3], S. Komamiya[24], R. Kowalewski[8], T. Kress[11], P. Krieger[6], J. von Krogh[11], P. Kyberd[13], G.D. Lafferty[16], H. Lafoux[8], R. Lahmann[17], W.P. Lai[19], J. Lauber[8], J.G. Layter[4], P. Leblanc[18], A.M. Lee[31], E. Lefebvre[18], D. Lellouch[26], C. Leroy[18], J. Letts[2], L. Levinson[26], S.L. Lloyd[13], F.K. Loebinger[16], G.D. Long[17], B. Lorazo[18], M.J. Losty[7], X.C. Lou[8], J. Ludwig[10], A. Luig[10], M. Mannelli[8], S. Marcellini[2], C. Markus[3], A.J. Martin[13], J.P. Martin[18], T. Mashimo[24], W. Matthews[25], P. Mättig[3], U. Maur[3], J. McKenna[29], T.J. McMahon[1], A.I. McNab[13], F. Meijers[8], F.S. Merritt[9], H. Mes[7], A. Michelini[8], R.P. Middleton[20], G. Mikenberg[26], D.J. Miller[15], R. Mir[26], W. Mohr[10], A. Montanari[2], T. Mori[24], M. Morii[24], U. Müller[3], B. Nellen[3], B. Nijjhar[16], S.W. O'Neale[1], F.G. Oakham[7], F. Odorici[2], H.O. Ogren[12], N.J. Oldershaw[16], C.J. Oram[28,a], M.J. Oreglia[9], S. Orito[24], F. Palmonari[2], J.P. Pansart[21], G.N. Patrick[20], M.J. Pearce[1], P.D. Phillips[16], J.E. Pilcher[9], J. Pinfold[30], D.E. Plane[8], P. Poffenberger[28], B. Poli[2], A. Posthaus[3], T.W. Pritchard[13], H. Przysiezniak[30], M.W. Redmond[8], D.L. Rees[8], D. Rigby[1], M.G. Rison[5], S.A. Robins[13], D. Robinson[5], N. Rodning[30], J.M. Roney[28], E. Ros[8], A.M. Rossi[2], M. Rosvick[28], P. Routenburg[30], Y. Rozen[8], K. Runge[10], O. Runolfsson[8], D.R. Rust[12], M. Sasaki[24], C. Sbarra[2], A.D. Schaile[8], O. Schaile[10], F. Scharf[3], P. Scharff-Hansen[8], P. Schenk[4], B. Schmitt[3], M. Schröder[8], H.C. Schultz-Coulon[10], P. Schütz[3], M. Schulz[8], C. Schwick[27], J. Schwiening[3], W.G. Scott[20], M. Settles[12], T.G. Shears[5], B.C. Shen[4], C.H. Shepherd-Themistocleous[7], P. Sherwood[15], G.P. Siroli[2], A. Skillman[15], A. Skuja[17], A.M. Smith[8], T.J. Smith[28], G.A. Snow[17], R. Sobie[28], S. Söldner-Rembold[10], R.W. Springer[30], M. Sproston[20], A. Stahl[3], M. Starks[12], C. Stegmann[10], K. Stephens[16],

J. Steuerer[28], B. Stockhausen[3], D. Strom[19], P. Szymanski[20], R. Tafirout[18], H. Takeda[24], T. Takeshita[24], P. Taras[18], S. Tarem[26], M. Tecchio[9], P. Teixeira-Dias[11], N. Tesch[3], M.A. Thomson[8], O. Tousignant[18], S. Towers[6], M. Tscheulin[10], T. Tsukamoto[24], A.S. Turcot[9], M.F. Turner-Watson[8], P. Utzat[11], R. Van Kooten[12], G. Vasseur[21], P. Vikas[18], M. Vincter[28], A. Wagner[27], D.L. Wagner[9], C.P. Ward[5], D.R. Ward[5], J.J. Ward[15], P.M. Watkins[1], A.T. Watson[1], N.K. Watson[7], P. Weber[6], P.S. Wells[8], N. Wermes[3], B. Wilkens[10], G.W. Wilson[27], J.A. Wilson[1], V-H. Winterer[10], T. Wlodek[26], G. Wolf[26], S. Wotton[11], T.R. Wyatt[16], A. Yeaman[13], G. Yekutieli[26], M. Yurko[18], V. Zacek[18], W. Zeuner[8], G.T. Zorn[17].

[1]School of Physics and Space Research, University of Birmingham, Birmingham B15 2TT, UK
[2]Dipartimento di Fisica dell' Università di Bologna and INFN, I-40126 Bologna, Italy
[3]Physikalisches Institut, Universität Bonn, D-53115 Bonn, Germany
[4]Department of Physics, University of California, Riverside CA 92521, USA
[5]Cavendish Laboratory, Cambridge CB3 0HE, UK
[6]Carleton University, Department of Physics, Colonel By Drive, Ottawa, Ontario K1S 5B6, Canada
[7]Centre for Research in Particle Physics, Carleton University, Ottawa, Ontario K1S 5B6, Canada
[8]CERN, European Organisation for Particle Physics, CH-1211 Geneva 23, Switzerland
[9]Enrico Fermi Institute and Department of Physics, University of Chicago, Chicago IL 60637, USA
[10]Fakultät für Physik, Albert Ludwigs Universität, D-79104 Freiburg, Germany
[11]Physikalisches Institut, Universität Heidelberg, D-69120 Heidelberg, Germany
[12]Indiana University, Department of Physics, Swain Hall West 117, Bloomington IN 47405, USA
[13]Queen Mary and Westfield College, University of London, London E1 4NS, UK
[15]University College London, London WC1E 6BT, UK
[16]Department of Physics, Schuster Laboratory, The University, Manchester M13 9PL, UK
[17]Department of Physics, University of Maryland, College Park, MD 20742, USA
[18]Laboratoire de Physique Nucléaire, Université de Montréal, Montréal, Quebec H3C 3J7, Canada
[19]University of Oregon, Department of Physics, Eugene OR 97403, USA
[20]Rutherford Appleton Laboratory, Chilton, Didcot, Oxfordshire OX11 0QX, UK
[21]CEA, DAPNIA/SPP, CE-Saclay, F-91191 Gif-sur-Yvette, France
[22]Department of Physics, Technion-Israel Institute of Technology, Haifa 32000, Israel
[23]Department of Physics and Astronomy, Tel Aviv University, Tel Aviv 69978, Israel
[24]International Centre for Elementary Particle Physics and Department of Physics, University of Tokyo, Tokyo 113, and Kobe University, Kobe 657, Japan
[25]Brunel University, Uxbridge, Middlesex UB8 3PH, UK
[26]Particle Physics Department, Weizmann Institute of Science, Rehovot 76100, Israel
[27]Universität Hamburg/DESY, II Institut für Experimental Physik, Notkestrasse 85, D-22607 Hamburg, Germany
[28]University of Victoria, Department of Physics, P O Box 3055, Victoria BC V8W 3P6, Canada
[29]University of British Columbia, Department of Physics, Vancouver BC V6T 1Z1, Canada
[30]University of Alberta, Department of Physics, Edmonton AB T6G 2J1, Canada
[31]Duke University, Dept of Physics, Durham, NC 27708-0305, USA

[32]Technische Hochschule Aachen, III Physikalisches Institut, Sommerfeldstrasse 26-28, D-52056 Aachen, Germany

[a]Also at TRIUMF, Vancouver, Canada V6T 2A3
[b] Royal Society University Research Fellow

1 Introduction

The production of hadrons in the decay of the Z^0 gauge boson involves the fragmentation stage, that is, the transition of coloured partons into colourless hadrons. No theoretical description exists yet for this process. Instead, a variety of phenomenological models has been developed. At the Z^0 energies the two most successful models are the string fragmentation model, incorporated in the JETSET program [1], and the cluster fragmentation scheme that is part of the HERWIG program [2]. Both programs were developed for centre-of-mass energies from 10 GeV to about 40 GeV and were tested extensively there [3]. More recently these programs have also been tuned, individually by each LEP experiment, to accommodate various inclusive features of the hadronic decays of the Z^0. Details of this procedure for the OPAL experiment are given in Ref. [4]. The study of the production and correlations of strange particles has been, and is, an important tool in the tests of the fragmentation models because these particles can be identified with high purity and large statistics over a wide momentum range. Since LEP came into operation, strange particle production, in particular inclusive K^0 production, has been studied in Z^0 decays by all four LEP collaborations [5, 6, 7, 8].

In addition to the single inclusive hadron properties it is also of interest to study the correlated production of two hadrons, in particular the so called Bose-Einstein Correlations (BEC). These have been investigated in pairs of identical pions over a wide energy range and for many different initial state reactions [9]. In contrast to that only few studies were reported on the BEC in charged and neutral kaon pairs in hadronic collisions [10, 11, 12, 13] and in e^+e^- annihilation at LEP [7, 14, 15].

In this paper we update with higher statistics two previous OPAL publications on the production of single K_S^0 and K_S^0-pairs. The current analysis is based on about 1.25×10^6 hadronic Z^0 decays recorded with the OPAL detector at LEP in 1990–92 as compared to the former paper on K^0 production [5] which used the data collected in 1990 (140 000 hadronic Z^0 decays) and the study of $K_S^0 K_S^0$ correlations [14] that used 750 000 events collected in 1990–1991.

The OPAL detector and the selection of the K_S^0 mesons are described in Section 2. We present in Section 3 the measurement of the K^0 rate and its differential cross section. In the same section we also relate our results to the predictions of fragmentation models and to previous studies of K^0 and $K^\pm$ production in Z^0 decays. Section 4 is devoted to a discussion of Bose-Einstein Correlations in the $K_S^0 K_S^0$ system and describes both the method and the experimental results. These findings are further compared to former analyses of BEC in charged and neutral kaon pairs. Finally, a summary and conclusions are presented in Section 5.

2 OPAL detector and data selection

2.1 The OPAL detector

The OPAL detector is designed to measure outgoing particles coming from e^+e^- annihilation at high energies. Details concerning the OPAL detector and its performance are given elsewhere [16]. Here we will describe briefly only those detector elements pertinent to the present analysis, namely the central tracking chambers.

These consist of a precision vertex detector, a large jet chamber and additional z-chambers surrounding the jet chamber. The vertex detector, a 1 m long cylindrical drift chamber of 470 mm diameter, surrounds the beam pipe and consists of an inner layer of 36 cells each

with 12 sense wires and an outer layer of 36 small angle (4°) stereo cells each with 6 sense wires. The jet chamber has a length of 4 m and a diameter of 3.7 m. It is divided into 24 sectors, each equipped with 159 sense wires ensuring a large number of measured points even for particles emerging from a secondary vertex. The z-chambers consist of 24 drift chambers, 4 m long, 50 cm wide and 59 mm thick. They are subdivided into 8 cells each with 6 sense wires perpendicular to those of the jet chamber and provide a precise measurement of the z coordinate along the beam direction[1]. They cover polar angles from 44° to 136° and 94% of the azimuthal angular range. All the chambers are contained in a solenoid providing an axial magnetic field of 0.435 T. The combination of these chambers leads to a momentum resolution of $\sigma_{p_t}/p_t \approx \sqrt{0.02^2 + (0.0015 \cdot p_t)^2}$ (p_t is the transverse momentum with respect to the beam direction in GeV/c), where the first term represents the contribution from multiple scattering [18].

2.2   Data selection

The present study was carried out with an integrated luminosity of about 45.9 pb^{-1} collected from 1990 to 1992 at centre-of-mass energies on and around the Z^0 mass. The criteria used to select hadronic Z^0 decays were based on the energy deposited in the electromagnetic calorimeter and the charged multiplicity in the tracking chambers and were described previously in Ref. [17]. The selection accepts $(98.4 \pm 0.4)\%$ of the multihadronic events while the remaining background, such as e$^+$e$^- \rightarrow \tau^+\tau^-$, is estimated to be at the level of less than 0.2%. In addition, we have accepted only multi-hadron events recorded while the jet and z-chambers were fully operational. After this selection 1 258 785 hadronic Z^0 decay events remained for the analysis.

K$_S^0$ selection

The method for selecting K$_S^0$ decays into $\pi^+\pi^-$ was slightly modified with respect to Refs. [5] and [14]. It started by systematically pairing tracks of opposite charge. These tracks had to fulfil the following conditions:

- a minimum transverse momentum of 150 MeV/c with respect to the beam direction;

- either more than 40 jet chamber hits or more than 25% of the geometrically possible jet chamber hits (but at least 20 hits);

- more than 3 z-chamber hits or a reconstructed end point inside the jet chamber, determined by using the last wire with a hit [18].

The latter requirement ensured a good mass resolution by improving the measurement of the polar angle.

Intersection points of track pairs in the plane perpendicular to the beam axis were considered to be secondary vertex candidates. Additional cuts were then imposed on them.

- The radial distance from the intersection point to the primary vertex had to be larger than 1 cm and smaller than 150 cm;

---

[1]A right-handed coordinate system is adopted by OPAL, where the x axis points to the centre of the LEP ring, and positive z is along the electron beam direction. The angles θ and ϕ are the polar and azimuthal angles, respectively.

- the reconstructed momentum vector of the K_S^0 candidate in the plane perpendicular to the beam axis had to point to the beam axis within $2°$;

- if the secondary vertex was reconstructed inside the jet-chamber volume, the radius of the first jet-chamber hit associated with either of the two tracks had to be less than 3 cm from the secondary vertex;

- if the secondary vertex was not reconstructed inside the jet-chamber volume, the radial distance of the charged track to the beam axis at the point of closest approach was required to exceed 3 mm;

- all track-pairs which passed these cuts were refitted in 3 dimensions with the constraint that they originate from a common vertex;

- pairs with an invariant mass of less than 100 MeV/c^2, when assuming both tracks to be electrons, were taken to be from photon conversions and were rejected;

- pairs with an invariant mass of less than 1125 MeV/c^2, when assuming the higher momentum track to be a proton (antiproton) and the lower momentum track to be a pion, were taken to be $\Lambda \to p\pi^-$ ($\overline{\Lambda} \to \overline{p}\pi^+$) decays and were rejected.

In the case where both intersections of the track pair passed these cuts, the one closer to the beam axis was taken.

The mass distribution of the reconstructed K_S^0 decays is shown in Fig. 1 assuming both tracks to be pions. To determine the K^0-parameters, mass and width, the distribution was fitted with a Gaussian shape plus a polynomial expression for the background (not shown in Fig. 1). The measured K^0 mass value obtained was (497.1 ± 0.1) MeV/c^2, in reasonable agreement[2] with the world average of (497.672 ± 0.031) MeV/c^2 [19]. The width obtained, $\sigma = (7.2 \pm 0.1)$ MeV/c^2, corresponds to our experimental mass resolution. The peak contains $182\,186 \pm 521$ K_S^0. All errors are statistical only.

3 K^0 production

3.1 Experimental procedure

In order to extract the number of K_S^0 so as to determine the K^0 cross section, it is necessary to estimate the amount of background under the signal peak and to correct for the detection efficiency. The signal was divided into 20 bins of the scaled energy x_E (defined as $x_E = 2 \cdot E_{K^0}/\sqrt{s}$, where $\sqrt{s}$ is the centre-of-mass energy) in the range $0.0114 \leq x_E \leq 0.8$. No significant K_S^0 signal is observed outside this x_E range. As an example, four of the 20 bins are shown in Fig. 2. In order to determine the background under the K_S^0 signal, polynomial fits to the mass spectrum were performed in each bin with the signal region (see below) excluded. To determine the number of K_S^0 per bin, the entries in the mass range from 450 MeV/c^2 to 550 MeV/c^2 (or from 400 MeV/c^2 to 600 MeV/c^2 for K_S^0 momentum larger than 5.7 GeV/c) were summed up and the background obtained from the fitted polynomial function was subtracted.

---

[2]The difference between the measured K_S^0 mass and the world average can be accounted for by the uncertainty in the mean value of the OPAL magnetic field and in the energy loss of the pions in the detector material.

This was followed by an efficiency correction performed separately in each x_E bin. The detection efficiency was defined as

$$\epsilon = \frac{N_{\text{reconstructed}}^{K_S^0 \to \pi^+\pi^-}}{N_{\text{generated}}^{K_S^0 \to \pi^+\pi^-}} \quad . \tag{1}$$

The efficiency was calculated using a sample of 1 million JETSET events[3] that were passed through a detailed simulation [20] of the OPAL detector and subjected to the same analysis chain as the real data. The detection efficiency is shown in Fig. 3 as a function of x_E. It shows a maximum of 27% at x_E of about 0.1. At high x_E, the efficiency is limited by the requirement of 40 jet chamber hits which cannot be met by K_S^0 decaying too far from the beam axis. Apart from the track cut at small transverse momentum, the decrease at low x_E is mainly due to the cut on the radial distance from the K_S^0 decay point to the primary vertex.

After correcting the data for the unobserved decay into $\pi^0\pi^0$ and for K_L^0 production, the differential cross section $(1/\sigma_{\text{had}})(d\sigma/dx_E)$ for K^0 production[4] was obtained as a function of x_E and is shown in Fig. 4a and Table 1. To determine the total K^0 rate, the momentum spectrum was integrated and JETSET was used to extrapolate over the unobserved momentum region. The last contribution was estimated to be 0.4% of the total rate. The corrected rate was found to be 1.990 ± 0.006 (stat.) K^0 per hadronic event in agreement with our previously published value of $2.10 \pm 0.02 \pm 0.14$ [5].

3.2   Systematic errors

In the study of the systematic error we distinguish between the systematic error of the overall normalization, that affects only the measurement of the K^0 rate, and a "bin–by–bin" error. This latter error quantifies the uncertainty in the shape of the differential cross section by defining a band around the measured points through a common systematic error. Within this band the shape may be distorted while retaining the measured K^0 rate. As sources of systematic error we consider the following contributions (shown in Table 2):

1. To estimate the systematic uncertainty arising from resolution differences between our data and the detector simulation, the K_S^0 selection cuts were varied. We determined the resulting error to be 0.9% on the K^0 rate and 2.9% bin–by–bin.

2. The uncertainty in the background subtraction described above was determined by varying the fit range and the mass range. Also, instead of a polynomial fit, a sideband method was used to calculate the background under the signal. The result was reproduced within 1.8% of the total rate and within 2.9% in each bin.

3. A relative uncertainty of 10% was attributed to the extrapolation over the unobserved momentum region due to differences in the predictions of JETSET and HERWIG.

4. The statistical error of the efficiency calculation results in a systematic uncertainty of the rate of 0.2%.

---

[3]The fragmentation parameters of the JETSET and HERWIG programs were tuned to describe the global event shapes as measured by OPAL [4]. Whenever referring to the generators throughout this paper, these tuned versions were used.

[4]Both particle and antiparticle state are implied.

5. A source of possible systematic errors on the detection efficiency arises from the choice of the fragmentation model. For this study only events generated with the JETSET program were accessible in sufficient numbers. We can, however, get a rough estimate of the expected systematic error from a HERWIG sample of 480 000 events. The detection efficiency calculated from HERWIG events shows a relative difference of 3% with respect to the one calculated using JETSET. This difference is not x_E dependent. This study shows (see below) that the K^0 energy spectrum predicted by HERWIG is clearly too soft. Previous studies demonstrated that HERWIG failed to describe particle correlations [21], in particular the correlated production of strange particles [14, 22], in OPAL data. Therefore, we do not include this error in our quoted systematic uncertainty of the K^0 rate.

After adding the contribution from 1 to 5 in quadrature the resulting systematic uncertainties were found to be 2.0% on the integrated K^0 rate and 4.1% bin–by–bin (a momentum dependent bin–by–bin statistical error on the efficiency of 0.8 to 4.9% should be added to the bin–by–bin systematic error).

3.3 Comparison to models and to previous measurements

In the following our K^0 rate and the differential cross section for K^0 production are compared to model calculations, to the corresponding results from the other LEP experiments and also to the production of charged kaons.

In Table 3 the K^0 rate is compared to the previously published measurements at Z^0 energies and to the predictions of the JETSET and HERWIG models. There is good agreement between the measurements within their errors. The JETSET prediction of 2.13 K^0 per event exceeds our result of 1.99 K^0 per event, and HERWIG overestimates the K^0 production by predicting a rate of 2.34. It is worth pointing out that each experiment quotes different rate estimates from the models due to differences in tuning, as can be seen in Table 3. A comparison of the shape of the differential cross section with the model prediction is shown in Fig. 4 where the K^0 rate of both generators was normalized to the measured K^0 rate. Fig. 4a shows the model predictions together with our measurements while Fig. 4b plots the bin–by–bin difference between each model and our data in units of the combined statistical and bin–by–bin systematic error of the data points. As can be seen, the predicted K^0 spectrum is clearly too soft in both models, more so in HERWIG than in JETSET.

As mentioned above, we have used as input to the high statistics detector simulation sample a JETSET version that was tuned to describe the global event shapes [4]. Attempts to tune JETSET to improve the agreement between predicted and measured particle inclusive rates can lead to a better agreement for the K^0 rate but are not successful in eliminating the discrepancy in the shape of the differential cross section.

In Fig. 5 and in Table 4 the differential cross section is presented as a function of $\xi = \ln(1/x_p)$, where $x_p = 2 \cdot p/\sqrt{s}$. This representation is especially suited to exhibit deviations between different data sets. The distribution shows the expected Gaussian shape in the region of the maximum [23]. In the framework of gluon momentum calculations in the modified leading log approximation (MLLA) [24] and assuming local parton-hadron duality (LPHD) [25], the position of the maximum of the differential cross section is of particular interest. A Gaussian fit to our data, motivated in Ref. [23], in the range of $|\xi - \xi_{max}| < 1.2$ yields $\xi_{max}^{K^0} = 2.71 \pm 0.04$ and is shown in Fig. 5. This value is lower than our previous one [5] of $\xi_{max}^{K^0} = 2.91 \pm 0.04$, as determined by a fit to the data using the MLLA "limited spectrum" expression [26]. However,

if instead of the MLLA expression a Gaussian shape is fitted to our previously published values, a peak position of $\xi_{max}^{K^0} = 2.82 \pm 0.06$ is found, consistent with the result of this study. In Fig. 5 our ξ distribution is also compared to the published results of the other LEP experiments. The agreement within errors between the various measurements of the differential cross sections is reasonable.

Finally, it is of interest to compare the results for neutral kaon production to the measurement of charged kaon production in this experiment [27]. In Table 5 the measured rates and the maxima of the ξ spectrum are given and compared to the predictions of the Monte Carlo generators. The measured difference between the integrated rates for charged and neutral kaon production is 0.43 ± 0.14 where the statistical and systematic errors are added in quadrature. A value larger than zero is expected due to the preferred decay of some particles, such as the $\phi(1020)$, into charged kaons compared to their decay into neutral kaons. Our value is larger than those of JETSET and HERWIG[5]. Note that in e^+e^- annihilation at lower energies, where charm and bottom production is less significant, the difference between the $K^\pm$ and K^0 rates was found to be consistent with zero [19]. The ξ distributions are compared in Fig. 6a. Good agreement between the shape of the distributions can be seen, in particular in Fig. 6b, where the $K^\pm$ rate was scaled to the measured K^0 rate. The predicted values of $\xi_{max}^{K^0,K^\pm}$ are too high in both generators, confirming the observation that the calculated fragmentation is too soft for both neutral and charged kaons.

4   Bose-Einstein correlations in the $K_S^0 K_S^0$ system

4.1   The method

Following our previous work [14] we used the Lorentz-invariant variable Q [28], the four momentum difference of the K_S^0 pair, which we here give as

$$Q^2 = M^2 - 4m^2 \ , \tag{2}$$

where M^2 is the invariant mass squared of the two kaons and m is the rest mass of each of them. The correlation function was then defined as

$$C(Q) = \frac{\rho(Q)}{\rho_0(Q)} \ , \tag{3}$$

where $\rho(Q)$ is the measured Q distribution for two K_S^0 mesons and $\rho_0(Q)$ is the Q distribution in the absence of BEC which we will refer to as the reference sample distribution.

Here one should note that in the decay of $Z^0 \rightarrow K_S^0 K_S^0 + hadrons$ one cannot determine if the kaons originated from identical bosons ($K^0 K^0$ or $\bar{K}^0 \bar{K}^0$) or if they are the product of a $K^0 \bar{K}^0$ boson-antiboson pair. From a sample of Monte Carlo generated events, to be described later, we have estimated that about 2/3 (3/4 for $Q < 1$ GeV) of our data sample of two K_S^0 events originate from a $K^0 \bar{K}^0$ pair and the rest from pairs of $K^0 K^0$ or $\bar{K}^0 \bar{K}^0$ mesons.

However, even in the case where the $K_S^0 K_S^0$ originate from a boson-antiboson pair, it has been shown in Refs. [14, 29, 30] that a BEC-like effect should be present. In fact, one can write the probability amplitude for a given charge conjugation eigenvalue C of the $K^0 \bar{K}^0$ system as:

$$\left| K^0; \bar{K}^0 \right\rangle_{C=\pm1} = \frac{1}{\sqrt{2}} \left| K^0(\vec{p}); \bar{K}^0(-\vec{p}) \right\rangle \ \pm \ \frac{1}{\sqrt{2}} \left| \bar{K}^0(\vec{p}); K^0(-\vec{p}) \right\rangle \ , \tag{4}$$

---

[5]Particle decays in our HERWIG version are modelled as in JETSET.

where $\vec{p}$ is the three-momentum vector defined in the $K^0\bar{K}^0$ centre-of-mass system. In the limit of $\vec{p} = 0$ ($Q = 0$), where the BEC should be maximal, Eq. 4 reads

$$\left|K^0; \bar{K}^0\right\rangle_{C=\pm 1} = \frac{1}{\sqrt{2}} \left|K^0(0); \bar{K}^0(0)\right\rangle \pm \frac{1}{\sqrt{2}} \left|\bar{K}^0(0); K^0(0)\right\rangle . \qquad (5)$$

This means that at $Q = 0$ the probability amplitude for the C = -1 state (odd ℓ values) is zero, whereas that of the state C = $+1$ (even ℓ values) is maximal. As is well known, the K^0 and the $\bar{K}^0$ bosons are described in terms of the two CP eigenstates, the K_S^0 with CP=+1 and the K_L^0 with CP=-1. Therefore, the $K_S^0 K_S^0$ and $K_L^0 K_L^0$ pairs are in a C = $+1$ state, whereas the $K_S^0 K_L^0$ pairs form a C = -1 state. From this it follows that, as Q approaches zero, an enhancement should be observed in the number of $K_S^0 K_S^0$ pairs and $K_L^0 K_L^0$ pairs whereas a depletion should occur in the number of $K_S^0 K_L^0$ pairs.

It is worthwhile to note that Eqs. 4 and 5 do hold for any $S\bar{S}$ pair, where S is a spinless boson. By defining the two possible states of the $S\bar{S}$ system through the even and odd ℓ states, rather than by the charge conjugation eigenvalues, a universal behaviour of the correlation function $C(Q)$ as a function of Q can be obtained [30] which covers also the identical boson case where only even ℓ states are allowed. This behaviour is shown schematically in Fig. 7 for the $K^0\bar{K}^0$, $K^0 K^0$ and $\bar{K}^0\bar{K}^0$ systems, where the even ℓ branch is the one expected for our $K_S^0 K_S^0$ data sample.

4.2 Experimental results

In order to reduce the background in the $K_S^0 K_S^0$ pair sample for the BEC analysis a cut on the measured mass of the K_S^0 candidate of $\pm$ 25 MeV/c^2 from the mean fitted value was introduced. This cut reduced the background to $(11 \pm 1)\%$, as calculated from the polynomial fit to the data, coming mainly from accidentally reconstructed secondary vertices and from some (about 0.5%) misidentified Λ-hyperons. The estimated background in the K_S^0 pair candidates sample, which hereafter will be referred to as $K_S^0 K_S^0$ pairs, was then $(21 \pm 1)\%$. In this way the data sample consisted of a total of 16 166 events containing 18 767 $K_S^0 K_S^0$ pairs.

The mass distribution, M_{KK}, of these $K_S^0 K_S^0$ pairs is shown in Fig. 8a. This distribution, which reaches its maximum near threshold, is seen to decrease smoothly as M_{KK} increases. In particular, unlike our findings with lower statistics [14], no indication is observed for the presence of the two $J^{PC} = 2^{++}$ resonances, $f_2'(1525)$ and $f_J(1710)$, in our current data. Two lower mass resonances, the $f_0(980)$ and $a_0(980)$, established through their decays to $\pi\pi$ and $\eta\pi$ respectively, are known to exist below the $K\bar{K}$ threshold. In principle, their decays can contribute to the $K_S^0 K_S^0$ mass distribution in the neighbourhood of the $K\bar{K}$ threshold. To estimate this contribution one requires knowledge of their production rate in Z^0 decays, their decay rate to $K\bar{K}$, and a model to describe the $K\bar{K}$ mass spectrum above threshold. Presently none of these factors are known with sufficient certainty. Furthermore, the former analyses of the $K\bar{K}$ decay mode have not addressed the question of a BEC enhancement in the $K_S^0 K_S^0$ channel.

To construct the correlation function $C(Q)$ it is necessary to have a reference sample distribution $\rho_0(Q)$ which should simulate the data distribution $\rho(Q)$, shown in Fig. 8b (full circles), in all its features except the BEC. As the reference sample we chose a Monte Carlo sample of 1.5×10^6 events which were generated with the JETSET program with the BEC option switched off. The events were passed through a detailed detector simulation and analyzed with the same programs as our data events. To verify that the Monte Carlo events are suited to use as a ref-

erence sample we have checked that those features of K_S^0 pairs which are relatively insensitive to the BEC effect were in good agreement with the data.

The correlation function, $C(Q)$, was obtained by dividing the data distribution by the reference sample distribution, shown in Fig. 8b, which was normalized to the total number of $K_S^0 K_S^0$ data pairs within the range of $0.6 \leq Q \leq 2$ GeV. This range was chosen so as to exclude the region where the BEC effect is expected. The resulting $C(Q)$ distribution is given in Table 6 and shown in Fig. 9a.

To extract the values of λ and R_0, we fitted via the minimum χ^2 method the following expression to the data, assuming a Gaussian shape of the particle source [9, 14, 31]:

$$C(Q) = N(1 + \mathrm{f}(Q)\lambda e^{-Q^2 R^2})(1 + \delta Q) , \qquad (6)$$

where N is a normalization factor and the parameter R is related to the boson emitter size R_0 in fm through the relation $R_0 = \hbar c R$. The parameter λ, often called the strength or chaoticity parameter, measures the strength of the effect and can vary between 0 and 1. In order to keep λ as the strength parameter only for the boson under study, one introduces a function $\mathrm{f}(Q)$ that should account for the background effects and their possible Q dependence. Monte Carlo studies showed that the background was essentially independent of Q and consequently $\mathrm{f}(Q)$ was set to 0.79, corresponding to the 21% background in our $K_S^0 K_S^0$ pair sample. The δ term accounts for the rise of $\mathrm{C}(Q)$ at large Q values due to long range two-particle correlations.

As the reference fit we chose three free parameters: λ, R_0 and δ. The normalization factor N was determined by the requirement that the area under the fitted $C(Q)$ curve be equal to that given by the data points. This fit yielded

$$\lambda = 1.14 \pm 0.23 \qquad R_0 = (0.76 \pm 0.10) \ \mathrm{fm} \qquad \delta = (0.10 \pm 0.05) \ \mathrm{GeV}^{-1} \ .$$

The correlation function and the reference fit are shown in Fig. 9a. Since we saw no indication for the presence of the $\mathrm{f}_2'(1525)$ and $\mathrm{f}_J(1710)$ resonances in the invariant mass distribution of the K_S^0-pairs, the full Q-range of $0 \leq Q \leq 2$ GeV was used in the fit. Unlike our previous results [14] the data do not yield a δ value consistent with zero. This may indicate the presence of long range correlations, such as energy conservation, phase space constraints and strangeness compensation [31]. For comparison we also fitted the correlation function with a 4-parameter fit (λ, R_0, δ, N), a 3-parameter fit (λ, R_0, N) and a 2-parameter fit (λ, R_0). The results of these fits are shown in Table 7. All fits have acceptable values for $\chi^2/\mathrm{d.o.f.}$ and result in consistent values for the parameters λ and R_0.

4.3   Systematic errors

To estimate the dependence of our results on the K_S^0 selection criteria we have repeated the analysis after varying these criteria within plausible ranges. The results of the corresponding 3-parameter fits are summarized in Table 8. We have changed the cut on the reconstructed mass of the K_S^0 over the range from $\pm$ 10 MeV/c^2 to $\pm$ 40 MeV/c^2 (row [a] in Table 8) and estimated the systematic uncertainty from the standard deviation of the differences to the reference fit. The track selection was changed by limiting the acceptance range to tracks with a polar angle between 44° and 136° (row [b]). To examine the dependence of the parameters on the Q range chosen for the normalization and the fit, we proceeded as follows. First, we used the limited Q-range 0 to 1.1 and 1.6 to 2 GeV (row [c]) to exclude the range of possible influence of the $\mathrm{f}_2'(1525)$ and $\mathrm{f}_J(1710)$ resonances. Then we used for $\mathrm{f}(Q)$, instead of a constant,

11

a linear function in Q, namely f(Q)=0.76 + 0.03·Q (row [d]). This slope is derived from Monte Carlo studies of the background under the K_S^0 peak and we chose the maximum slope allowed within one standard deviation from the mean value. We estimated the systematic error of the sources [b]–[d] from the difference of the fit result to the reference fit. We further assumed the individual deviations, given in Table 8, to be independent and thus, by adding them in quadrature, we obtained an uncertainty of ± 0.21 and ± 0.08 fm for λ and R_0, respectively.

As observed in previous BEC studies of charged pion pairs, an important source of systematic errors stems from the particular choice of the reference sample. These systematic errors were estimated in the di-pion studies from a comparison of several acceptable reference samples. Here, however, we are limited to only one reference sample and have therefore adopted the following method to estimate the systematic uncertainties. Event samples were generated with the JETSET program by varying, one at a time, its free parameters within one standard deviation of the optimized values. The limits for the following parameters were given in Ref. [32]. They are: the QCD cut-off parameter Λ_{QCD}, the Q_0 parameter, which specifies the minimum parton virtuality to which partons may evolve, σ_q, which controls the transverse momentum spectrum of hadrons and the parameter a, which determines the longitudinal momentum spectrum. The higher value for the ratio of strange vector mesons to vector plus pseudoscalar mesons is derived from the mean value and the errors given in Ref. [33], while the lower value was the one presented by this experiment in Ref. [34]. Finally we used for the strangeness suppression factor γ_s/γ_u the lower value given in Ref. [34].

The resulting Q distributions were then divided by the standard generated distribution before detector simulation to obtain Q-dependent weights to modify the standard reference sample with full detector simulation. With these modified distributions we repeated the BEC analysis. The values of the changed parameters and the variation of the fit results are given in Table 9. Although we find no numerical evidence for a significant variation, we quote the standard deviation of the differences to the reference fit as the systematic uncertainty. We assume the deviations to be uncorrelated and, by adding them in quadrature, obtain uncertainties of ± 0.24 for λ and ± 0.08 fm for the R_0 value. Finally we added in quadrature the contributions from the variation of the selection and the fit conditions to the reference sample uncertainties yielding a total systematic uncertainty of ±0.32 for λ and ±0.11 fm for R_0.

4.4 Comparison to previous measurements

In Table 10 we present our λ and R_0 values together with former results from BEC studies of kaon pairs which have extracted an R_0 value[6], including the recent $K_S^0 K_S^0$ results from the LEP experiments. For comparison we also give the LEP results for the BEC in like-sign charged pion pairs. In comparing our results with those listed in Table 10 one should keep the following in mind:

1. The λ values for the BEC obtained in hadronic reactions are in general lower than those obtained in e$^+$e$^-$ annihilation [9].

2. No systematic errors are given in Refs. [10], [11] and [13] and therefore the errors quoted in the table are statistical only.

---

[6]In addition to the λ and R_0 values given in Table 10, recent analyses [35, 36] studied the $K^\pm K^\pm$ BEC in heavy ion collisions. These yielded similar results to those obtained for $\pi^\pm \pi^\pm$ pairs in the same reactions. In these heavy ion collisions R_0 is known to increase as $A_{projectile}^{1/3}$ (see e.g. Zajc in Ref. [31]).

3. In the BEC analyses of charged pions it was observed that those experiments which have used the variables q_t, q_0, proposed in Ref. [37], tend to yield higher values of R_0 than those obtained through the analysis of the Q variable [9]. In fact, the R_0 values obtained for charged kaons are larger than our measurement. Our result for R_0 is consistent with that reported by the BEC study of $K^0_S K^0_S$ pairs, described in Ref. [13]. That experiment, however, did not extract a value for the chaoticity parameter λ.

4. The recently published $K^0_S K^0_S$ BEC analyses by DELPHI [15] and ALEPH [7] have followed rather closely the first published OPAL work [14] in both their method and choice of reference sample. However, both analyses perform a subtraction of the $f_0(980)$ decay contribution to the low mass $K^0_S K^0_S$ enhancement. To this end, they used the $K\bar{K}$ branching ratio given by the Particle Data Group [38] and the mean $f_0(980) \to \pi^+\pi^-$ multiplicity of 0.10 ± 0.04 with $x_E(f_0(980)) > 0.1$ as measured by DELPHI in Z^0 hadronic decays [39]. We did not adopt this approach for the reasons given in Section 4.2. Instead, we have looked for evidence of the presence of the $f_0(980)$ and $a_0(980)$ in the K^+K^- mass spectrum [34]. At this time we cannot draw any conclusions due to the limited sensitivity. Consequently, although no reliable quantitative estimate is possible from these analyses, we cannot presently exclude that a part of the enhancement is in fact due to scalar meson decays.

   In addition, rather than looking at the BEC effect in an inclusive sample, DELPHI used JETSET to correct for those events in which the $K^0_S K^0_S$ pairs are the decay product of the heavy charm and bottom quarks.

5. Finally it should also be mentioned that a meaningful comparison of the λ and R_0 values given in Table 10 is difficult because the various experiments have used different types of reference samples and different methods to offset the background and account for Coulomb effects.

Notwithstanding these reservations, our values for the OPAL data are in good agreement with our previously published values of $\lambda = 1.12 \pm 0.33 \pm 0.29$ and $R_0 = (0.72 \pm 0.17 \pm 0.19)$ fm [14] and those presented recently by the DELPHI and ALEPH collaborations. This is also illustrated in Fig. 9b in a 2-dimensional plot of λ versus R_0 where the contours represent confidence levels of 39%, 86% and 99% as calculated from the statistical errors.

Finally it is of interest to compare our results for the dimension of the K^0_S source and its chaoticity parameter to those found for the pion source in e^+e^- annihilation at the same energy. In this case, a direct comparison is possible since the type of reaction and the chosen observables are identical. As can be seen from Table 10, our values for λ and R_0 are similar to those obtained for like-sign charged pions.

5 Summary and conclusions

The production and Bose-Einstein correlations of neutral kaons in e^+e^- annihilation at $\sqrt{s} \simeq M_{Z^0}$ have been studied in $1\,258\,785$ hadronic events recorded with the OPAL detector at LEP during 1990–92.

The K^0 yield was found to be $1.99 \pm 0.01 \pm 0.04$ K^0 per hadronic event. This rate is lower than the JETSET and HERWIG predictions. The differential cross sections are found to be too soft in both JETSET and HERWIG. A similar trend was observed by this experiment in a study of the production of charged kaons [27]. Both the rate and the differential cross section as a

13

function of $\ln(1/x_p)$ agree well with the other published measurements of K^0 production at Z^0 energies.

An enhancement at small Q values is seen in our sample of $K_S^0 K_S^0$ pairs originating from a mixed sample of $K^0 \bar{K}^0$ and $K^0 K^0$ ($\bar{K}^0 \bar{K}^0$) pairs. If we attribute this enhancement entirely to the Bose-Einstein correlations, a fit to our data yields

$$\lambda = 1.14 \pm 0.23 \pm 0.32 \qquad R_0 = (0.76 \pm 0.10 \pm 0.11) \text{ fm.}$$

These values are in good agreement with our former results and with the published BEC studies at Z^0 energies.

Acknowledgements:

References

[1] T. Sjöstrand, Comp. Phys. Comm. **39** (1986) 347;
T. Sjöstrand and M. Bengtsson, Comp. Phys. Comm. **43** (1987) 367.

[2] G. Marchesini and B.R. Webber, Nucl. Phys. **B310** (1988) 461;
G. Marchesini, B.R. Webber et al., Comp. Phys. Comm. **67** (1992) 465.

[3] For a study of strange particle production in e^+e^- annihilation at lower energies see e.g.
CELLO Collaboration, H. Behrend et al., Z. Phys. **C46** (1990) 397, and references therein.

[4] OPAL Collaboration, P.D. Acton et al., Z. Phys. **C58** (1993) 387.

[5] OPAL Collaboration, G. Alexander et al., Phys. Lett. **B264** (1991) 467.

[6] L3 Collaboration, M. Acciarri et al., Phys. Lett. **B328** (1994) 223.

[7] ALEPH Collaboration, D. Buskulic et al., Z. Phys. **C64** (1994) 361.

[8] DELPHI Collaboration, P. Abreu et al., CERN-PPE/94-130, submitted to Z. Phys. **C**.

[9] For a recent summary of BEC results see e.g. E. A. De Wolf, to be published in the
Proceedings of the XXIV International Symposium on Multiparticle Dynamics, Eds. A.
Giovannini, S. Lupia and R. Ugoccioni, World Scientific, Singapore.

[10] T. Åkesson et al., Phys. Lett. **B155** (1985) 128.

[11] M. Aguilar-Benitez et al., Z. Phys. **C54** (1992) 21.

[12] D. Bertrand et al., Nucl. Phys. **B128** (1977) 365.

[13] A.M. Cooper et al., Nucl. Phys. **B139** (1978) 45.

[14] OPAL Collaboration, P.D. Acton et al., Phys. Lett. **B298** (1993) 456.

[15] DELPHI Collaboration, P. Abreu et al., Phys. Lett. **B323** (1994) 242.

[16] OPAL Collaboration, K. Ahmet et al., Nucl. Instr. and Meth. **A305** (1991) 275.

[17] OPAL Collaboration, G. Alexander et al., Z. Phys. **C52** (1991) 175.

[18] O. Biebel et al., Nucl. Instr. and Meth. **A323** (1992) 169.

[19] Review of Particle Properties, Phys. Rev. **D50** (1994) part I.

[20] J. Allison et al., Nucl. Instr. and Meth. **A317** (1992) 47.

[21] OPAL Collaboration, P.D. Acton et al., Phys. Lett. **B276** (1992) 547.

[22] OPAL Collaboration, P.D. Acton et al., Phys. Lett. **B305** (1993) 415.

[23] Y.L. Dokshitzer, V.A. Khoze and S.I. Troyan, J. Phys. G: Nucl. Part. Phys. **17** (1991)
1481;
Y.L. Dokshitzer, V.A. Khoze and S.I. Troyan, Z. Phys. **C55** (1992) 107.

[24] Y.L. Dokshitzer and S.I. Troyan, Leningrad preprint LNPI-922 (1984) (in Russian);
Y.I. Azimov, Y.L. Dokshitzer, V.A. Khoze and S.I. Troyan, Z. Phys. **C27** (1985) 65.

[25] D. Amati and G. Veneziano, Phys. Lett. **B83** (1979) 87;
Y.I. Azimov et al., Phys. Lett. **B165** (1985) 147.

[26] V.A. Khoze, Y.L. Dokshitzer and S.I. Troyan, Lund preprint LU TP 90-12 (1990).

[27] OPAL Collaboration, R. Akers et al., Z. Phys. **C63** (1994) 181.

[28] G. Goldhaber et al., Phys. Rev. Lett. **3** (1959) 181;
G. Goldhaber et al., Phys. Rev. **120** (1960) 300.

[29] H. Lipkin, Phys. Rev. Lett. **69** (1992) 3700;
H. Lipkin, Phys. Lett. **B219** (1989) 474;
H. Lipkin, Argonne report ANL-HEP-PR-88-66.

[30] G. Alexander, Frascati preprint LNF-93-001(P);
G. Alexander, Tel-Aviv University preprint TAUP-2133-94, to be published in the Proceedings of the Int. Conf. on "Bose and the 20th Century Physics", 30 December 1993 – 5 January 1994, Calcutta, India.

[31] M. Gyulassy et al., Phys. Rev. **C20** (1979) 2267;
W. Hofmann, Lawrence Berkeley Laboratory preprint LBL 23108 (1987);
W.A. Zajc, in "Hadronic Multiparticle Production", P. Carruthers ed., World Scientific (1988) 235;
M.I. Podgoretskii, Sov. J. Part. Nucl. **20** (1989) 266.

[32] OPAL Collaboration, M.Z. Akrawy et al., Z. Phys. **C47** (1990) 505.

[33] W. Hofmann, Ann. Rev. Nucl. Part. Phys. **38** (1988) 279.

[34] OPAL Collaboration, P.D. Acton et al., Z. Phys. **C56** (1992) 521.

[35] Y. Akiba et al., Phys. Rev. Lett. **70** (1993) 1057.

[36] H. Beker et al., Z. Phys. **C64** (1994) 209.

[37] G.I. Kopylov and M.I. Podgoretskii, Sov. J. Nucl. Phys. **18** (1974) 336;
G.I. Kopylov and M.I. Podgoretskii, Sov. J. Nucl. Phys. **18** (1973) 656.

[38] Review of Particle Properties, Phys. Rev. **D45** (1992) part II.

[39] DELPHI Collaboration, P. Abreu et al., Phys. Lett. **B298** (1993) 236.

[40] G. D. Lafferty and T. R. Wyatt, Nucl. Instr. and Meth. **A355** (1995) 541

[41] ALEPH Collaboration, D. Decamp et al., Z. Phys. **C54** (1992) 75.

[42] DELPHI Collaboration, P. Abreu et al., Z. Phys. **C63** (1994) 17.

[43] OPAL Collaboration, P.D. Acton et al., Phys. Lett. **B267** (1991) 143.

Tables

x_E	x_{lw}	$(1/\sigma_{had})\ d\sigma/dx_E$				
0.0114 - 0.02	0.014	25.4	$\pm$	0.4	$\pm$	1.1
0.02 - 0.03	0.025	24.3	$\pm$	0.2	$\pm$	1.0
0.03 - 0.04	0.035	19.1	$\pm$	0.2	$\pm$	0.8
0.04 - 0.05	0.045	15.3	$\pm$	0.1	$\pm$	0.6
0.05 - 0.06	0.055	13.0	$\pm$	0.13	$\pm$	0.54
0.06 - 0.07	0.065	11.0	$\pm$	0.12	$\pm$	0.46
0.07 - 0.08	0.075	9.24	$\pm$	0.11	$\pm$	0.39
0.08 - 0.09	0.085	8.36	$\pm$	0.10	$\pm$	0.36
0.09 - 0.10	0.095	6.92	$\pm$	0.09	$\pm$	0.30
0.10 - 0.125	0.111	5.66	$\pm$	0.05	$\pm$	0.24
0.125 - 0.15	0.136	4.43	$\pm$	0.05	$\pm$	0.19
0.15 - 0.20	0.172	3.06	$\pm$	0.03	$\pm$	0.13
0.20 - 0.25	0.223	1.92	$\pm$	0.02	$\pm$	0.08
0.25 - 0.30	0.273	1.25	$\pm$	0.019	$\pm$	0.055
0.30 - 0.35	0.323	0.849	$\pm$	0.016	$\pm$	0.039
0.35 - 0.40	0.373	0.572	$\pm$	0.014	$\pm$	0.028
0.40 - 0.45	0.424	0.389	$\pm$	0.012	$\pm$	0.020
0.45 - 0.50	0.474	0.250	$\pm$	0.009	$\pm$	0.014
0.50 - 0.60	0.549	0.161	$\pm$	0.005	$\pm$	0.009
0.60 - 0.80	0.689	0.050	$\pm$	0.002	$\pm$	0.003

Table 1: *The differential cross section for K^0 production. The errors given are the statistical and bin–by–bin systematic errors. A normalization error of 2.0% should be added. The appropriate position of the data points within the x_E bins, x_{lw}, was determined according to the procedure given in Ref. [40].*

Source of systematic error	error on K^0 rate	bin–by–bin error
detector simulation	$\pm\ 0.9\%$	$\pm\ 2.9\%$
background subtraction	$\pm\ 1.8\%$	$\pm\ 2.9\%$
statistical error of efficiency	$\pm\ 0.2\%$	$\pm\ (0.8 - 4.9)\%$
unobserved momentum region	$\pm\ 0.04\%$	$\pm\ 0.0\%$
total syst. error on K^0 rate	$\pm\ 2.0\%$	

Table 2: *Systematic errors of the K^0 production rate.*

	K^0 rate		
Experiment	measured	JETSET	HERWIG
DELPHI [8]	$1.962 \pm 0.022 \pm 0.056$	1.965	—
L3 [6]	$2.04 \pm 0.02 \pm 0.14$	2.16	2.18
ALEPH [7]	2.061 ± 0.047	2.11	2.24
OPAL [this study]	$1.99 \pm 0.01 \pm 0.04$	2.13	2.34

Table 3: *Summary of K^0 production rates in Z^0 hadronic decays. Also given are the measurements of the other LEP experiments and the predictions of the Monte Carlo programs, tuned individually by each experiment.*

ξ	$(1/\sigma_{\mathrm{had}})\,\mathrm{d}\sigma/\mathrm{d}\xi$					ξ	$(1/\sigma_{\mathrm{had}})\,\mathrm{d}\sigma/\mathrm{d}\xi$				
0.2 - 0.4	0.025	$\pm$	0.002	$\pm$	0.001	3.0 - 3.2	0.667	$\pm$	0.007	$\pm$	0.036
0.4 - 0.6	0.061	$\pm$	0.002	$\pm$	0.003	3.2 - 3.4	0.645	$\pm$	0.008	$\pm$	0.034
0.6 - 0.8	0.111	$\pm$	0.003	$\pm$	0.006	3.4 - 3.6	0.574	$\pm$	0.008	$\pm$	0.031
0.8 - 1.0	0.177	$\pm$	0.004	$\pm$	0.010	3.6 - 3.8	0.517	$\pm$	0.008	$\pm$	0.027
1.0 - 1.2	0.267	$\pm$	0.005	$\pm$	0.014	3.8 - 4.0	0.459	$\pm$	0.008	$\pm$	0.024
1.2 - 1.4	0.346	$\pm$	0.005	$\pm$	0.018	4.0 - 4.2	0.356	$\pm$	0.008	$\pm$	0.019
1.4 - 1.6	0.421	$\pm$	0.006	$\pm$	0.022	4.2 - 4.4	0.291	$\pm$	0.009	$\pm$	0.015
1.6 - 1.8	0.510	$\pm$	0.006	$\pm$	0.027	4.4 - 4.6	0.194	$\pm$	0.008	$\pm$	0.011
1.8 - 2.0	0.576	$\pm$	0.006	$\pm$	0.031	4.6 - 4.8	0.128	$\pm$	0.009	$\pm$	0.007
2.0 - 2.2	0.628	$\pm$	0.006	$\pm$	0.034	4.8 - 5.0	0.094	$\pm$	0.008	$\pm$	0.005
2.2 - 2.4	0.679	$\pm$	0.007	$\pm$	0.036	5.0 - 5.2	0.090	$\pm$	0.009	$\pm$	0.005
2.4 - 2.6	0.702	$\pm$	0.007	$\pm$	0.037	5.2 - 5.4	0.040	$\pm$	0.006	$\pm$	0.002
2.6 - 2.8	0.710	$\pm$	0.007	$\pm$	0.038	5.4 - 5.6	0.034	$\pm$	0.008	$\pm$	0.002
2.8 - 3.0	0.696	$\pm$	0.007	$\pm$	0.037						

Table 4: *The measured ξ distribution for K^0 production. The errors given are the statistical and bin–by–bin systematic errors, not including an overall normalization error of 2.0%.*

	OPAL	JETSET	HERWIG
$K^{\pm}$ rate	2.42 ± 0.13	2.26	2.47
K^0 rate	1.99 ± 0.04	2.13	2.34
difference	0.43 ± 0.14	0.13	0.13
$\xi_{max}^{K^{\pm}}$	2.63 ± 0.04	2.77 ± 0.01	2.77 ± 0.01
$\xi_{max}^{K^0}$	2.71 ± 0.04	2.82 ± 0.01	2.82 ± 0.01

Table 5: *The integrated rate and ξ_{max} for charged [27] and neutral kaons measured in Z^0 decays. For the particle rates the statistical and systematic errors were added in quadrature while only the error of the fit is quoted for ξ_{max}.*

Q [GeV]	correlation function $C(Q)$	Q [GeV]	correlation function $C(Q)$
0.0 – 0.2	1.59 ± 0.19	1.1 – 1.2	1.02 ± 0.06
0.2 – 0.4	1.18 ± 0.06	1.2 – 1.3	0.97 ± 0.06
0.4 – 0.5	0.93 ± 0.06	1.3 – 1.4	1.13 ± 0.07
0.5 – 0.6	1.03 ± 0.06	1.4 – 1.5	1.10 ± 0.07
0.6 – 0.7	0.89 ± 0.05	1.5 – 1.6	1.00 ± 0.07
0.7 – 0.8	0.89 ± 0.05	1.6 – 1.7	1.03 ± 0.07
0.8 – 0.9	1.00 ± 0.05	1.7 – 1.8	0.93 ± 0.07
0.9 – 1.0	1.05 ± 0.06	1.8 – 1.9	0.94 ± 0.07
1.0 – 1.1	1.01 ± 0.06	1.9 – 2.0	1.09 ± 0.08

Table 6: *The measured correlation function $C(Q)$ in the range $0 \leq Q \leq 2$ GeV. The errors represent the combined statistical uncertainty of the data and the Monte Carlo samples.*

Type of Fit	χ^2/d.o.f.	λ	R_0 [fm]	δ [GeV^{-1}]	N
reference fit (λ, R_0, δ)	17.1/15	1.14 $\pm$0.23	0.76 $\pm$0.10	0.10 ± 0.05	1.00
4-parameter (λ, R_0, δ, N)	17.1/14	1.19 $\pm$0.34	0.76 $\pm$0.11	0.08 ± 0.05	0.93 ± 0.07
3-parameter (λ, R_0, N)	20.0/15	1.03 $\pm$0.32	0.83 $\pm$0.12	0.00	0.99 ± 0.02
2-parameter (λ, R_0)	20.5/16	1.05 $\pm$0.22	0.84 $\pm$0.11	0.00	1.00

Table 7: *Results of the χ^2 fits to $C(Q)$, as defined in Eq. 6, in the range of $0 \leq Q \leq 2$ GeV. The errors are statistical only.*

Fit conditions	$\Delta\lambda$	ΔR_0 [fm]
[a] K_S^0 mass cut	$\pm$ 0.17	$\pm$ 0.03
[b] modified track selection	$\pm$ 0.10	$\pm$ 0.07
[c] Q-range: 0 to 1.1 and 1.6 to 2 GeV	$\pm$ 0.05	$\pm$ 0.00
[d] f(Q)=0.76 + 0.03$\cdot Q$	$\pm$ 0.04	$\pm$ 0.00
total error	$\pm$ 0.21	$\pm$ 0.08

Table 8: *Systematic errors on the BEC analysis due to changes in the selection criteria and the fit conditions.*

JETSET parameter variation	$\Delta\lambda$	ΔR_0 [fm]
[a] $0.28 \leq \Lambda_{QCD} \leq 0.31$ GeV	$\pm$ 0.10	$\pm$ 0.03
[b] $0.70 \leq Q_0 \leq 1.80$ GeV	$\pm$ 0.09	$\pm$ 0.02
[c] $0.32 \leq \sigma_q \leq 0.40$ GeV	$\pm$ 0.10	$\pm$ 0.04
[d] $0.13 \leq a \leq 0.30$	$\pm$ 0.11	$\pm$ 0.03
[e] $0.43 \leq (\frac{V}{V+P})_S \leq 0.68$	$\pm$ 0.12	$\pm$ 0.03
[f] $0.245 \leq \gamma_s/\gamma_u \leq 0.30$	$\pm$ 0.07	$\pm$ 0.04
total error	$\pm$ 0.24	$\pm$ 0.08

Table 9: *Systematic uncertainties in the BEC analysis due to changes in the parameters of the* JETSET *reference sample which control the momentum distribution of hadrons.*

Measurement		Reaction	$\sqrt{s}$ [GeV]	Method	λ	R_0 [fm]
$K^\pm K^\pm$	[10]	$pp, \overline{p}p, \alpha\alpha$	53 - 126	q_t, q_0	0.58 ± 0.31	2.4 ± 0.9
$K^\pm K^\pm$	[11]	pp	27.4	q_t, q_0	0.57 ± 0.26	1.87 ± 0.33
$K_S^0 K_S^0$	[13]	$\overline{p}p$	2.0	q_t, q_0	——	0.9 ± 0.2
$K_S^0 K_S^0$	[15]	e^+e^-	91	Q	$1.13 \pm 0.54 \pm 0.23$	$0.90 \pm 0.19 \pm 0.10$
$K_S^0 K_S^0$	[7]	e^+e^-	91	Q	$0.96 \pm 0.21 \pm 0.40$	$0.65 \pm 0.07 \pm 0.15$
$K_S^0 K_S^0$	[this study]	e^+e^-	91	Q	$1.14 \pm 0.23 \pm 0.32$	$0.76 \pm 0.10 \pm 0.11$
$\pi^\pm \pi^\pm$	[41]	e^+e^-	91	Q	$0.51 \pm 0.04 \pm 0.11$	$0.65 \pm 0.04 \pm 0.16$
$\pi^\pm \pi^\pm$	[42]	e^+e^-	91	Q	$1.06 \pm 0.05 \pm 0.16$	$0.49 \pm 0.01 \pm 0.05$
$\pi^\pm \pi^\pm$	[43]	e^+e^-	91	Q	$1.08 \pm 0.05 \pm 0.14$	$0.93 \pm 0.02 \pm 0.15$

Table 10: *Results for λ and R_0 obtained from BEC studies of like-sign charged kaons and K_S^0 pairs using the Goldhaber variable Q and the variables q_t and q_0 of Kopylov and Podgoretskii [37]. These are defined as follows: if $q = p_1 - p_2 = (q_0, \vec{q})$ then q_t denotes the component of $\vec{q}$ perpendicular to $\vec{p_1} + \vec{p_2}$, where $\vec{p_1}$, $\vec{p_2}$ and $\vec{q}$ are the three momenta vectors. For comparison are also shown the results for like-sign charged pions obtained by the LEP experiments.*

Figure Captions

Figure 1: The $\pi^+\pi^-$ invariant mass distribution of the K^0_S candidates.

Figure 2: The $\pi^+\pi^-$ invariant mass distribution of the K^0_S candidates in four selected bins of x_E.

Figure 3: The detection efficiency for $K^0_S \rightarrow \pi^+\pi^-$ as a function of its scaled energy x_E.

Figure 4: a) The differential cross section $(1/\sigma_{had})(d\sigma/dx_E)$ vs. x_E for K^0 production. The error bars show the combined statistical and bin–by–bin systematic contributions. An overall normalization error of 2.0% should be added.
b) The difference between the measured differential cross section and the generator predictions in units of the error of the data points.

Figure 5: The measured $\xi = \ln(1/x_p)$ distribution for K^0 production. The error bars show the combined statistical and bin–by–bin systematic contributions. An overall normalization error of 2.0% should be added. The line shows the result of a Gaussian fit to the spectrum. The OPAL measurement is compared to the published measurements of the other LEP experiments [6, 7, 8].

Figure 6: a) The measured $\xi = \ln(1/x_p)$ distributions of the OPAL charged [27] and neutral kaons. The error bars show the combined statistical and bin–by–bin systematic contributions. The line and the shaded area indicate the interpolation function used in the analysis of the $K^\pm$ and its one sigma range, respectively. An overall normalization error of 2.0% should be added for the K^0 analysis.
b) Same as a) where, for comparison, the $K^\pm$ rate is scaled to the K^0 rate.

Figure 7: Schematic behaviour of the correlation function $C(Q)$ as a function of Q for the $K^0\bar{K}^0$ system in the charge conjugation eigenvalue C= +1 (even ℓ) state and in the C= -1 (odd ℓ) state [30]. The sum of these two eigenvalue states is independent of Q and is represented by the dotted horizontal line.

Figure 8: a) The invariant mass distribution, M_{KK}, of the $K^0_S K^0_S$ pairs.
b) The Q distribution for the data (full circles) compared to the same distribution obtained from the Monte Carlo simulated events (histogram). The area under the Monte Carlo distribution is normalized to the data in the range $0.6 \leq Q \leq 2.0$ GeV. The statistical errors of the Monte Carlo sample are of about the same magnitude as those of the data.

Figure 9: a) The measured Bose-Einstein correlation function $C(Q)$. The solid line represents the best fit to the data using Eq. 6 with a 3-parameter χ^2 fit.
b) λ versus R_0. The full circle represents our best values. The contours show the allowed regions within one, two and three standard deviations of λ and R_0 (corresponding to confidence levels of 39%, 86%, and 99%, respectively), calculated from the statistical errors only. Published results from DELPHI [15] and ALEPH [7] are shown, with their statistical errors only, for comparison.
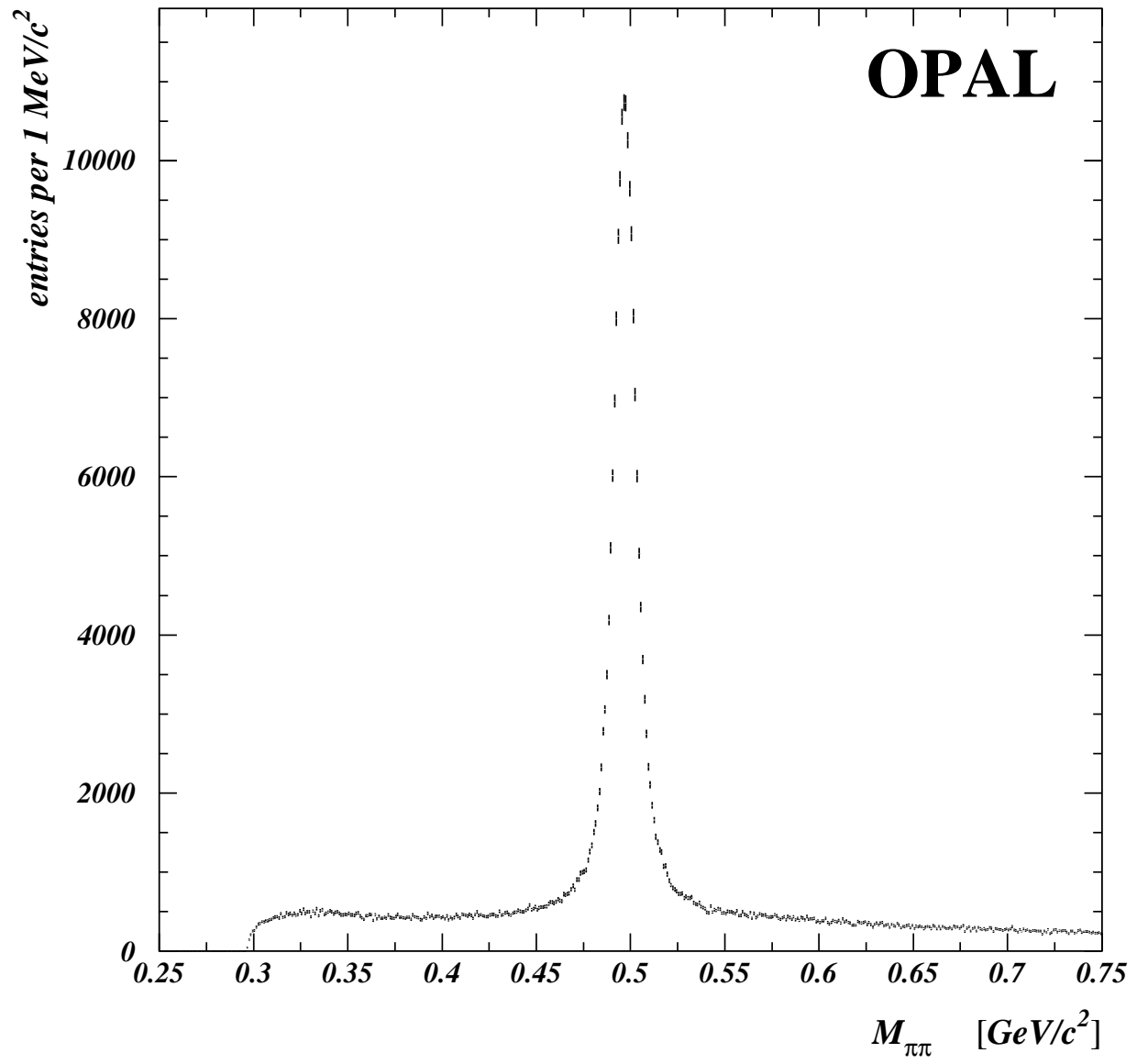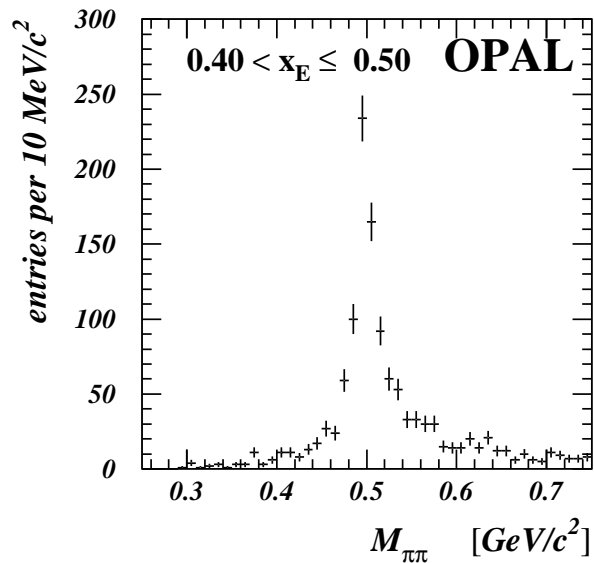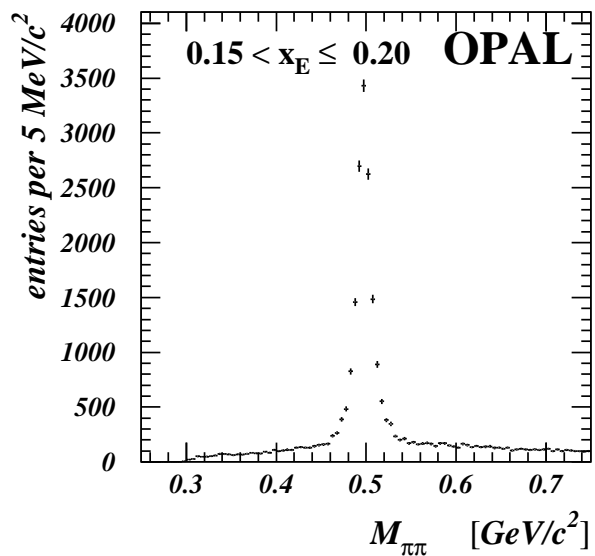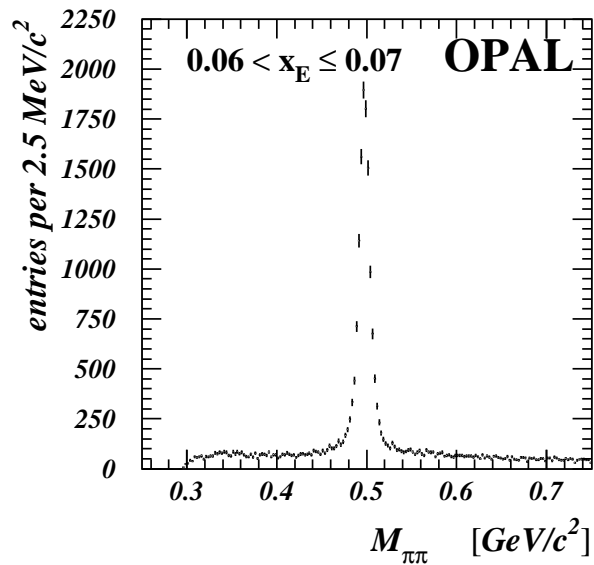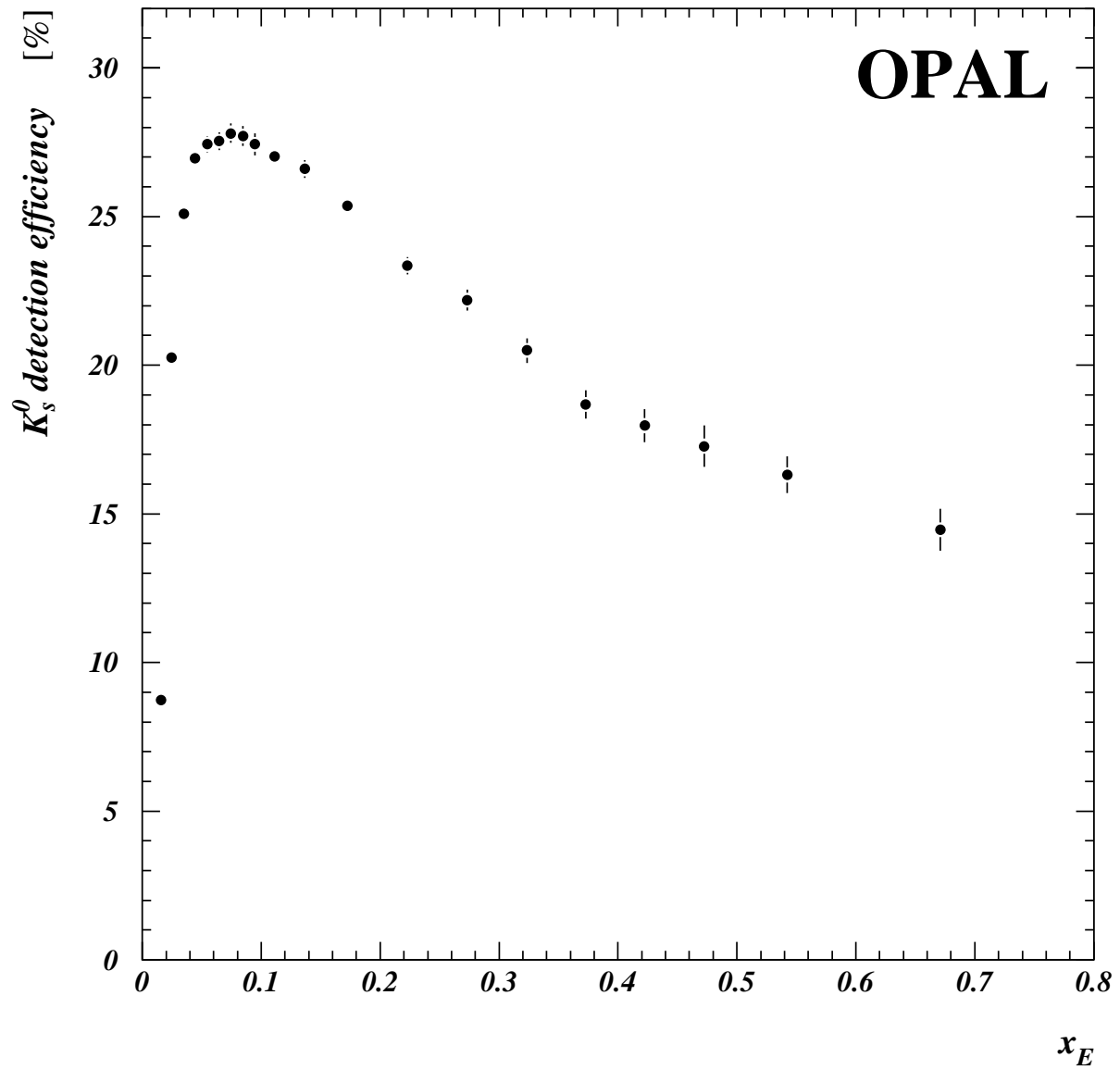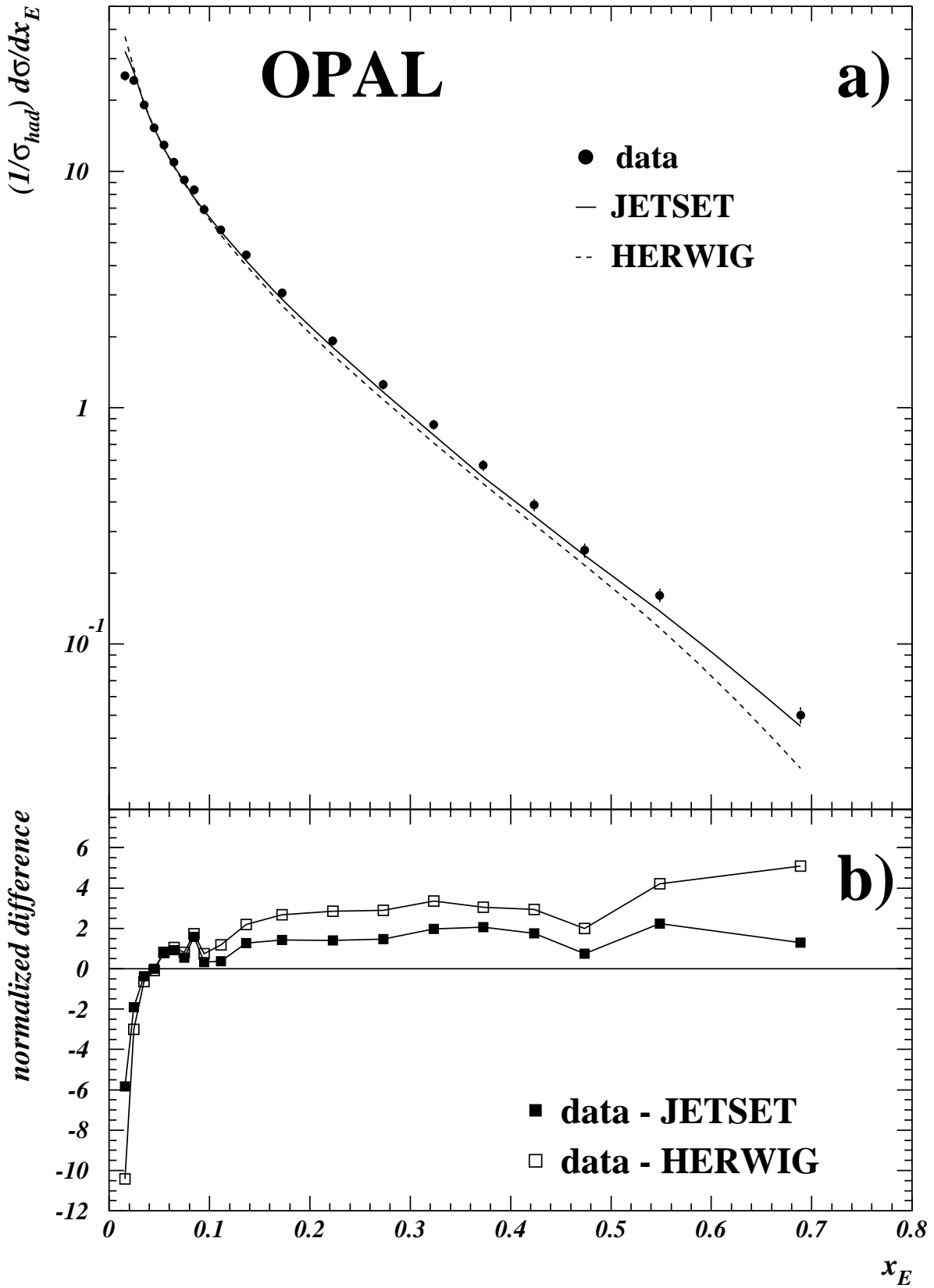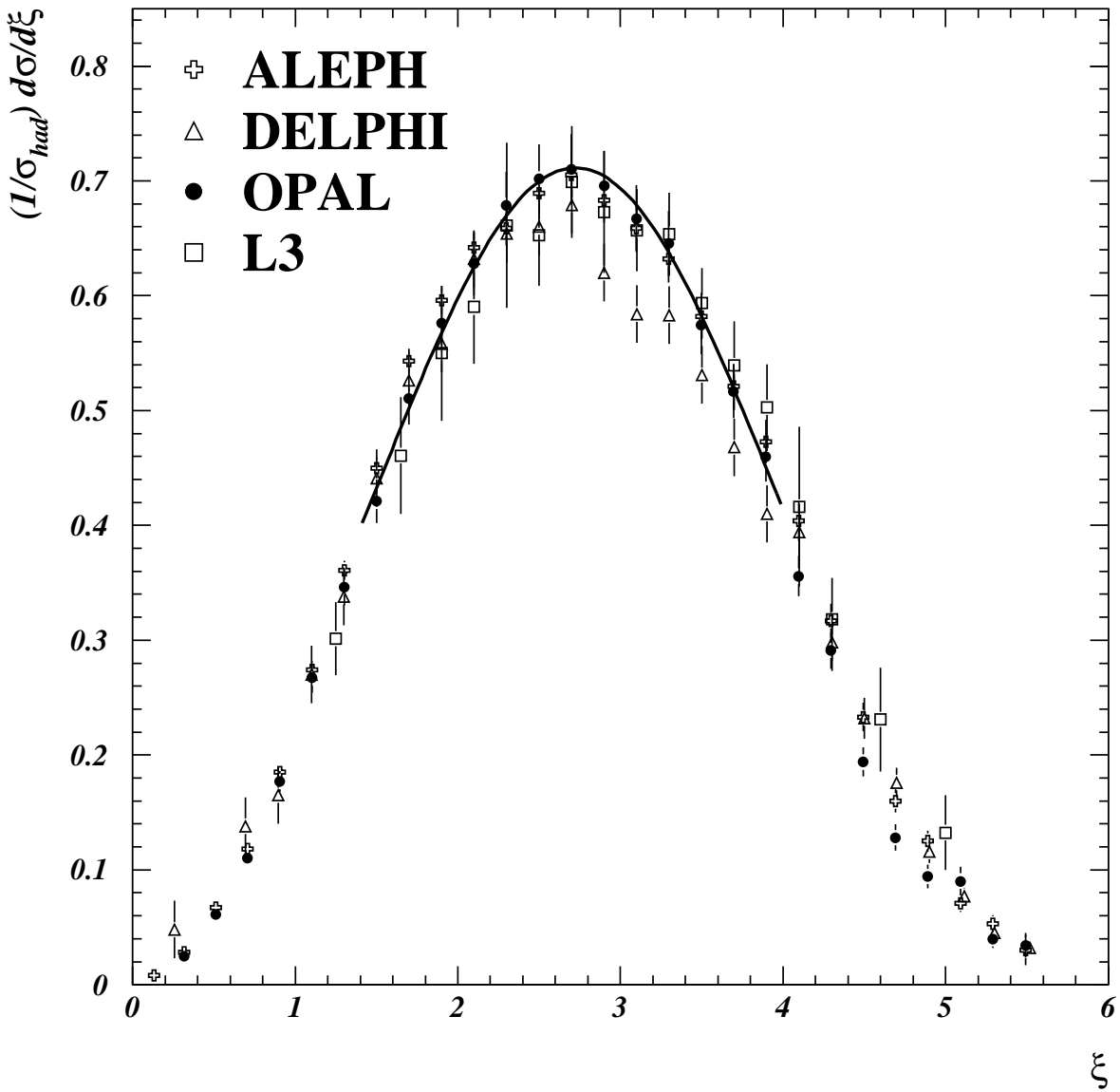
figure 1

figure 2
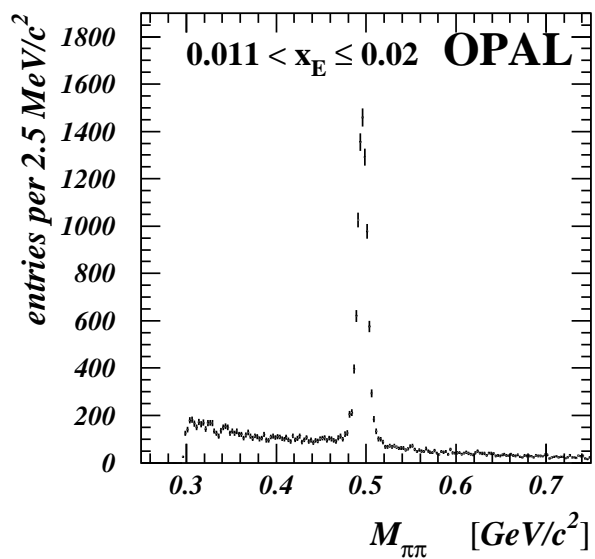
figure 3

figure 4

figure 5

figure 6
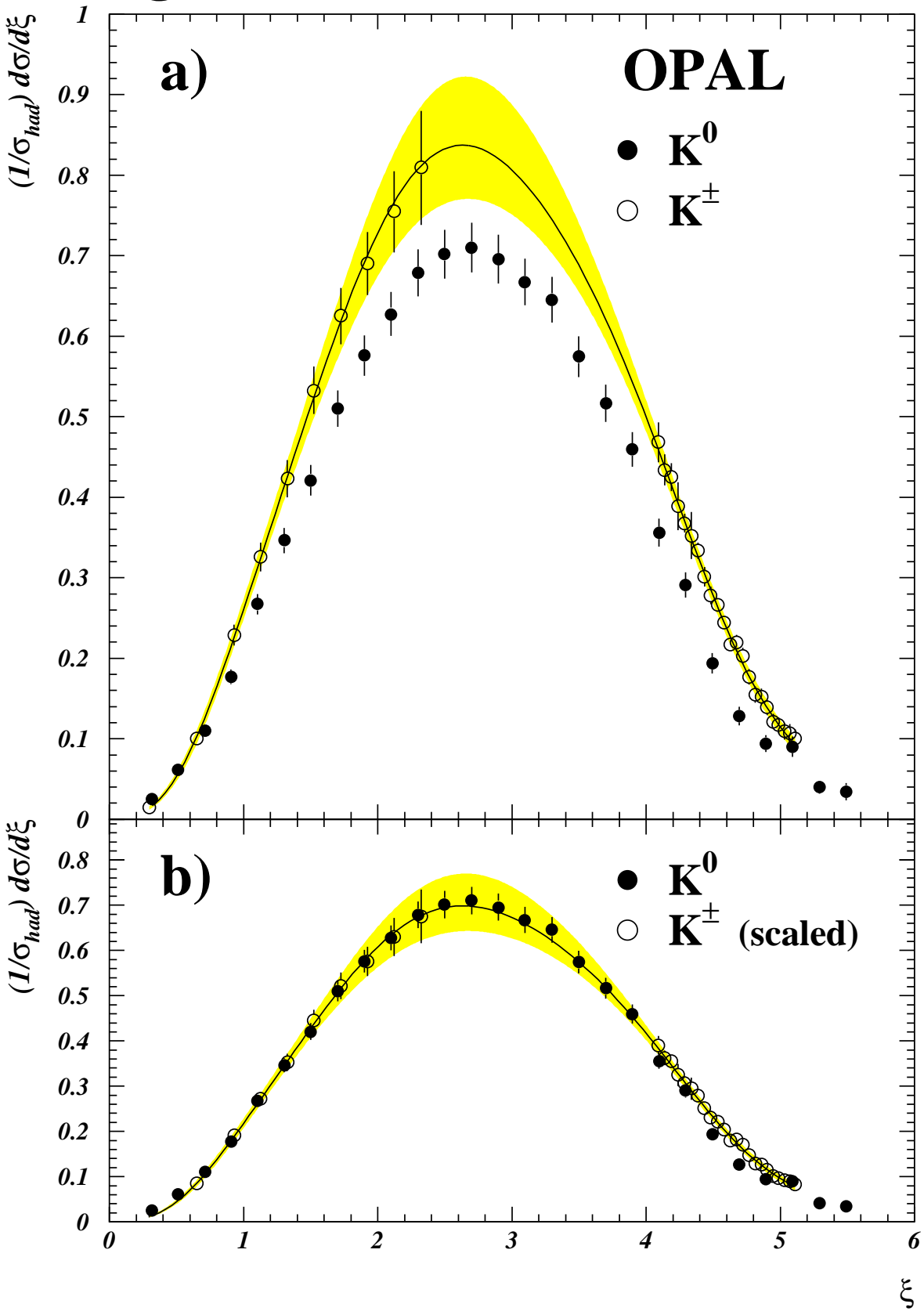
figure 7

figure 8

figure 9